Nitrogen content and isotopic composition of oceanic crust at a superfast spreading ridge: A profile in altered basalts from ODP Site 1256, Leg 206

Vincent Busigny, Christine Laverne, Magali Bonifacie

Geochemistry Geophysics Geosystems G3
AN ELECTRONIC JOURNAL OF THE EARTH SCIENCES
Published by AGU and the Geochemical Society

Article
Volume 6, Number 12
30 December 2005
Q12O01, doi:10.1029/2005GC001020
ISSN: 1525-2027

Nitrogen content and isotopic composition of oceanic crust at a superfast spreading ridge: A profile in altered basalts from ODP Site 1256, Leg 206

Vincent Busigny

Laboratoire de Géochimie des Isotopes Stables, UMR 7047, IPGP et Université Paris VII, 2 Place Jussieu, F-75252 Paris Cedex 05, France

Origins Laboratory, Department of the Geophysical Sciences, University of Chicago, 5734 South Ellis Avenue, Chicago, Illinois 60637, USA (busigny@geosci.uchicago.edu)

Christine Laverne

Laboratoire de Pétrologie Magmatique, Case 441, Université Paul Cézanne Aix-Marseille III, Faculté des Sciences et Techniques, Avenue Escadrille Normandie Niemen, F-13397 Marseille Cedex 20, France

Magali Bonifacie

Laboratoire de Géochimie des Isotopes Stables, UMR 7047, IPGP et Université Paris VII, 2 Place Jussieu, F-75252 Paris Cedex 05, France

[1] The present paper provides the first measurements of both nitrogen content and isotopic composition of altered oceanic basalts. Samples were collected from Ocean Drilling Program Site 1256 located at the eastern flank of the East Pacific Rise. Twenty-five samples affected by low temperature alteration were analyzed. They include moderately altered basalts together with veins and related alteration halos and host rocks, as well as unique local intensely altered basalts showing green (celadonite-rich) and red (iron oxyhydroxide-rich) facies. Nitrogen contents of moderately altered basalts range from 1.4 to 4.3 ppm and are higher than in fresh MORB. Their $\delta^{15}N$ values vary in a large range from +1.6 to +5.8‰. Veins, halos, and host rocks are all enriched in N relative to moderately altered basalts. Notably, veins show particularly high N contents (354 and 491 ppm) associated with slightly low $\delta^{15}N$ values (+0.4 and −2.1‰). The intensely altered red and green facies samples display high N contents of 8.6 and 9.7 ppm, respectively, associated with negative $\delta^{15}N$ values of −3.8 and −2.7‰. Detailed petrological examination coupled with N content suggests that N of altered basalts occurs as ammonium ion (NH_4^+) fixed in various secondary minerals (celadonite, K- and Na-feldspars, smectite). A body of evidence indicates that N is enriched during alteration of oceanic basalts from ODP Site 1256, contrasting with previous results obtained on basalts from DSDP/ODP Hole 504B (Erzinger and Bach, 1996). Nitrogen isotope data support the interpretation that N in metasomatizing fluid occurred as N_2, derived from deep seawater and likely mixed with magmatic N_2 contained in basalt vesicles.

Components: 10,988 words, 4 figures, 3 tables.

Keywords: nitrogen isotopes; ammonium; basalts; alteration processes; ODP Site 1256.

Index Terms: 1021 Geochemistry: Composition of the oceanic crust; 1039 Geochemistry: Alteration and weathering processes (3617); 1041 Geochemistry: Stable isotope geochemistry (0454, 4870).

Received 16 May 2005; **Revised** 9 September 2005; **Accepted** 21 October 2005; **Published** 30 December 2005.

Busigny, V., C. Laverne, and M. Bonifacie (2005), Nitrogen content and isotopic composition of oceanic crust at a superfast spreading ridge: A profile in altered basalts from ODP Site 1256, Leg 206, *Geochem. Geophys. Geosyst.*, *6*, Q12O01, doi:10.1029/2005GC001020.

Theme: Formation and Evolution of Oceanic Crust Formed at Fast Spreading Rates
Guest Editors: Damon A. H. Teagle and Doug Wilson

1. Introduction

[2] Nitrogen behaves as an insoluble element in basaltic melts generated at mid-ocean ridges (MOR). Several studies demonstrated that nitrogen solubility ($\sim 4.10^{-9}$ mol/g/atm) is very close to that of argon [e.g., *Marty et al.*, 1995; *Cartigny et al.*, 2001; *Miyazaki et al.*, 2004]. Nitrogen is thus strongly concentrated in gas vesicles formed by decompression of basaltic melts rising up to the surface. Subsequent escape of the gas from magmas via degassing process releases most N, leaving only traces of the amount initially incorporated during partial melting. Consequently total N concentrations in fresh basalts (i.e., N dissolved in glass and included in gas vesicles) are usually very low. The least degassed MOR basalt that has ever been analyzed (the popping-rock 2πD43) show a total N content of only 12 ppm and a part of this N may be inherited from surface contamination as shown by slightly low $^{40}Ar/^{36}Ar$ (i.e.,<6,200 [*Javoy and Pineau*, 1991]). Nitrogen dissolved in fresh degassed MORB glasses varies over a small range from 0.3 to 2.8 ppm and averages 1.1 ppm [*Sakai et al.*, 1984; *Exley et al.*, 1987; *Marty et al.*, 1995]. Isotopic compositions of this nitrogen show a large range from −4.6 to +7.9‰ [*Sakai et al.*, 1984; *Exley et al.*, 1987], but these data may present inherent problems related to the step-heating extraction technique [*Marty et al.*, 1995]. Nitrogen in fresh MORB glasses vesicles extracted by crushing experiments displays a large range of $\delta^{15}N$ values, between −8.9 and +6.5‰, which converge to ∼ −4‰ [*Javoy and Pineau*, 1991; *Marty and Humbert*, 1997; *Marty and Zimmermann*, 1999; *Nishio et al.*, 1999; *Cartigny et al.*, 2001]. Positive $\delta^{15}N$ values of MORB vesicles are variably interpreted as reflecting (1) occurrence of a sedimentary component in mantle source [*Marty and Humbert*, 1997], (2) contamination by recycled ''modern'' organic nitrogen [*Marty and Zimmermann*, 1999], or (3) isotopic fractionation during degassing process [*Cartigny et al.*, 2001].

[3] Contrasting with previous knowledge on fresh basalts, the fate of N during alteration of oceanic crust by seawater is very poorly documented. Only two studies estimated N content of altered basalts, but provide no data on their N isotopic composition [*Hall*, 1989; *Erzinger and Bach*, 1996]. One of these studies focused on the Hole 504B samples and argued that hydrothermal alteration induces a loss of N from rock to fluid [*Erzinger and Bach*, 1996]. The second one estimated N content of altered basalts from Cornubian (Southwest England) and concluded that N was enriched in rocks during alteration processes [*Hall*, 1989]. Although these opposite results may have strong implications on the global N geodynamic cycle, the reason for this discrepancy has not been elucidated yet. Systematic quantitative and isotopic analyses of N in altered oceanic crust are required to better constrain N behavior during hydrothermal alteration of oceanic basalts.

[4] The section of oceanic crust drilled at Ocean Drilling Program (ODP) Site 1256 during Leg 206 completed the initial phase of a planned multi-leg project to drill a complete in situ section that will extend through the lavas, the sheeted dikes and down to the gabbros. This project should (1) complement the present reference section of the oceanic crust provided by DSDP/ODP Hole 504B, which ends in the lower sheeted dikes, and (2) bring new constraints on seawater-oceanic crust interactions. In this framework, the present contribution provides N content and isotopic composition of low temperature altered basalts drilled at ODP Site 1256 during Leg 206. Coupling these data with detailed petrological observations, the speciation of N in altered basalts is discussed and suggested to occur mainly as ammonium ion. Low temperature alteration processes are shown to produce an enrichment of N fixed in basalts via interaction with fluids. The nature of supplied nitrogen is discussed using N isotope data.

2. Geological Background

[5] Ocean Drilling Program Site 1256 (6°44.2′N, 91°56.1′W) is located on the eastern flank of the

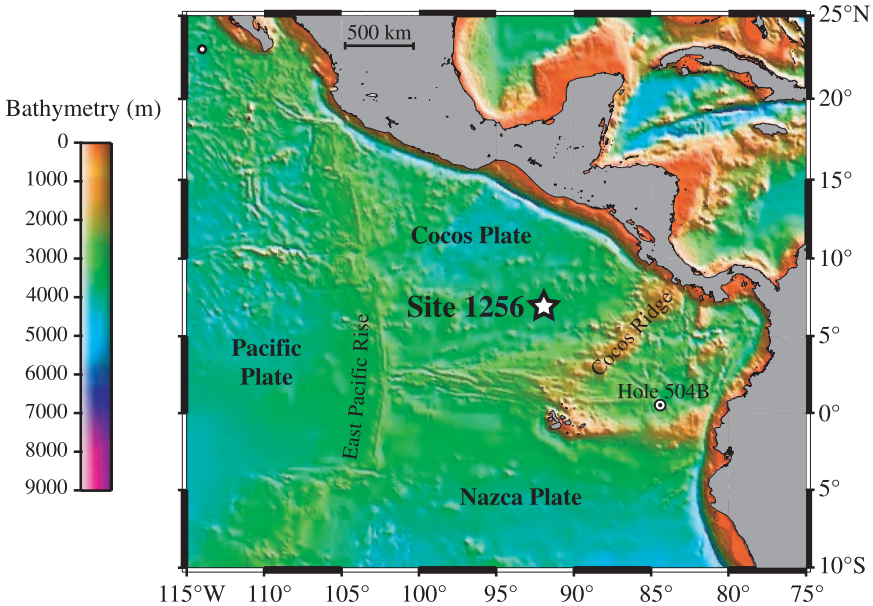

Figure 1. Bathymetric map showing the location of ODP Site 1256 in the Cocos Plate (modified after *Shipboard Scientific Party* [2003]). Location of DSDP/ODP Hole 504B is reported for comparison.

East Pacific Rise (Figure 1). It lies on ~15 Ma oceanic lithosphere of the Cocos plate under 3635 m of water in the Guatemala oceanic basin. ODP Site 1256 has been chosen in the hope to drill a complete section of oceanic crust because the crust at this site was accreted at a superfast spreading rate (~200–220 mm/yr [*Wilson*, 1996]) and the upper gabbros are predicted to occur at relatively shallow depth (1100–1300 mbsf [*Shipboard Scientific Party*, 2003]).

[6] Three pilot holes were cored at ODP Site 1256. Hole 1256B recovered a nearly complete section of 250.7 m of sediments overlying basement and Hole 1256C penetrated 88.5 m into the basement. Hole 1256D, located 30 m far from Holes 1256B and C, drilled more than 500 m of basalts (sheet flows, pillow lavas, hyaloclastites, massive lava flows and rare dikes). All samples analyzed in the present work were collected from Hole 1256D, except two samples from Hole 1256C. They experienced low-temperature alteration processes. However, contrasting with other DSDP/ODP holes, basalts sampled at ODP Site 1256 during Leg 206 are only slightly affected by low-temperature alteration. Notably, alteration by oxidizing seawater is much less common than in Hole 504B [*Shipboard Scientific Party*, 2003].

3. Sample Description: Petrological and Mineralogical Features

[7] The main alteration features of basalts investigated in this study are given in Table 1 and the chemical composition of their secondary minerals is presented in Table 2. Most of these basalts exhibit a dark gray background alteration (n = 15; Figures 2a and 2b). This type of alteration is the most common and abundant one throughout Holes 1256C and 1256D, and is interpreted as resulting from interaction of basalts with seawater at low-temperature and low water/rock ratio [*Shipboard Scientific Party*, 2003]. The alteration degree, corresponding to the amount of secondary minerals, is slight to moderate (2–20%). It does not vary with depth but is related to rock texture and primary mineralogy. Saponite (Table 2) and minor pyrite fill pore spaces and replace olivine. Among these 15 samples, some of them slightly differ from typical background altered ones: (1) sample 206-1256D-22R-2, 120–127 cm contains two thin (<0.2 mm) pyrite + brown smectite veinlets; (2) sample 206-1256D-27R-1, 130–137 cm contains large (up to 1 cm) connected alteration patches with pyrite and dark brown smectite; (3) sample 206-1256D-47R-2, 121–126 cm displays a pyrite veinlet, and pyrite crystals disseminated in the basalt adjacent to the vein; (4) in sample 206-1256D-69R-1, 24–33 cm, plagioclase phenocrysts are completely replaced by dark brown smectite; (5) in sample 206-1256D-74R-2, 102–111 cm, plagioclase phenocrysts are extensively replaced by secondary albite. The plagioclase replacement observed in Hole 1256D below 621 mbsf is interpreted as due to slightly higher temperatures than the overlying section or more evolved fluids

Table 1. Types of Alteration and Main Alteration Features of Samples From Site 1256[a]

Hole	Core Section	Interval, m	Rock Type	Secondary Minerals, %	Secondary Minerals	Plagioclase Replacement
1256C	4R-1	13–20	chert	-		-
1256C	8R-1	101–108	bckgrd alt.	-	sm	no
1256D	9R-4	90–97	bckgrd alt. (m.fl.)	-	sm, chl/m	no
1256D	12R-8	71–79	bckgrd alt. (m.fl.)	-	sm, tlc/sm	no
1256D	16R-1	88–95	bckgrd alt.	-	sm	no
1256D	22R-2	120–127	bckgrd alt.	-	sm, pyr	no
1256D	24R-1	132–139	bckgrd alt.	-	sm	no
1256D	26R-6	18–21	p. brwn host rock	8	sm, pyr, qtz	no
1256D	26R-6	18–21	brwn halo	12	Fe-oxhydr/phyll, *grn cpx*, *alb*	*alb*
1256D	26R-6	18–21	vein	100	mag, phyll	-
1256D	27R-1	130–137	bckgrd alt.	-	sm, pyr	no
1256D	32R-1	114.120	bckgrd alt.	-	sm	no
1256D	37R-1	36–43	bckgrd alt.	-	sm	no
1256D	41R-2	26–23	bckgrd alt.	-	sm	no
1256D	47R-2	121–126	bckgrd alt.	-	sm, pyr	no
1256D	52R-1	8–15	bckgrd alt.	-	sm	no
1256D	57R-2	118–127	blue-green facies	85	cel, sm, Fe-oxhydr, Ca-carb	KF + cel
1256D	57R-3	15–19	brick-red facies	85	Fe-oxhydr, cel, KF, Si-mal, Ca-carb	KF, Fe-hydrox, Ca-carb
1256D	57R-4	118–125	bckgrd alt.	-	sm	no
1256D	67R-1	47–50	p. brwn host rock	8	sm, Si-mal, alb	brwn sm + alb
1256D	67R-1	47–50	dark green halo	8	cel, hydgrt, Si-mal, sm	brwn sm
1256D	67R-1	47–50	vein	100	Fe-hydr, cel, Si-mal	-
1256D	69R-1	24–33	bckgrd alt.	-	sm	dk brwn sm
1256D	74R-2	102–111	bckgrd alt.	-	sm, alb, Si-mal	alb
BAS-206	-	-	composite	-	-	-

[a] Rock types: bckgrd alt., background alteration; m.fl., massive flow; p. brwn, pale brown. Secondary minerals: sm, smectite; chl/sm, interlayered or mixed layered chlorite/smectite; tlc/sm, interlayered or mixed layered talc/smectite; pyr, pyrite; Fe-oxhydr/phyll, mixture of iron oxyhydroxide and phyllosilicate; mag, magnetite; qtz, quartz; cel, celadonite; Ca-carb, calcium carbonate; KF, K-feldspar; alb, albite; Si-mal, Si-mineral; hydgrt, hydrogarnet. Plagioclase replacement: dk brwn, dark brown. Italics indicate minerals restricted to the narrow inner alteration halo of the brown halo (see text for explanation). The proportion of secondary minerals in samples affected by background alteration ranges from 2 to 20% (it has not been specifically estimated for each sample of this study).

[*Shipboard Scientific Party*, 2003]. Sample 206-1256C-4R-1, 13–20 cm is a chert from the sedimentary section of Hole 1256C. Sample BAS-206 is a composite powder corresponding to a mixture of various rubbles of basalts from Hole 1256D recovered in a junk basket.

[8] Alteration related to veins is manifested as different-colored halos along veins. Three types of alteration halos commonly occur in the section of Hole 1256D cored during Leg 206 and are typical features of upper oceanic crust altered at low temperature: (1) "black halos" either black, dark gray or dark green are characterized by the presence of celadonite, (2) "brown oxidized halos" which can exhibit various shades of brown, red, and orange, due to the presence of iron-oxyhydroxides, and (3) mixed halos resulting from partial or complete superimposition of brown halos on black halos.

[9] In order to study vein-related alteration, two samples were selected: 206-1256D-26R-6, 18–21 cm (containing a brown alteration halo) and 206-1256D-67R-1, 47–50 cm (containing a mixed alteration halo). The former one (Figure 2e) is crosscut by a dark brown vein composed, from the center to the edge, by finely crystallized orange-brown phyllosilicate (Table 2), iron-oxyhydroxides globules, and locally very abundant large aggregates of subhedral or anhedral magnetite crystals including scarce small green clinopyroxenes (Table 2). In the 1 mm thick contact zone between the vein and the adjacent 8 mm thick orange-brown alteration halo, secondary Na-feldspar occurs as small (<100 μm) isolated crystals or as partial or total replacement product of magmatic plagioclase (Table 2). In the orange-brown halo, thin section examination reveals general orange-brown staining of primary minerals, and abundant very dark brown iron oxyhydroxides (Table 2)

Table 2 (Representative Sample). Representative Chemical Analyses of Secondary Minerals of Samples From Site 1256[a] [The full Table 2 is available in the HTML version of this article at http://www.g-cubed.org.]

Analysis run	B4	B4	B6	B6	B6	B6	B6	B6	B5	B4	B5	B6	B6	B4	B4	B1	B1	B1	B1
Analysis number	269	275	3	129	4	15	19	141	73	278	76	10	8	217	218	66	78	75	76
Hole	1256D	1256D	1256D	1256D	1256D	1256D	1256D	1256D	1256D	1256D	1256D	1256D	1256D	1256D	1256D	1256D	1256D	1256D	1256D
Core section	26R-6	26R-6	26R-6	26R-6	26R-6	26R-6	26R-6	26R-6	26R-6	26R-6	26R-6	26R-6	26R-6	34R-4	34R-4	57R-3	57R-3	57R-3	57R-3
Interval, cm	18–21	18–21	18–21	18–21	18–21	18–21	18–21	18–21	18–21	18–21	18–21	18–21	18–21	37–40	37–40	0–1	0–1	0–1	0–1
Rock type	vn	vn	vn	vn	inn halo	inn halo	inn halo	brw halo	brw halo	host-R	host-R	host-R	host-R	bck grd	bckgrd	red fac	red fac	red fac	red fac
Mineral type	phyll	phyll	phyll	cpx	sec F	mag pl	sec F	mag cpx	ox/phyll	phyll	phyll	phyll	mag pl	sm	sm	cel	cel	sec KF	sec KF
Mineral color	or	brw	brw	gr					brw	brw	brw	brw		brwish	brwish	gr	gr	c	c
Mineral location									int	int	rep ol	ves		int	int	int	rep ol	rep pl	rep pl
SiO_2	43.88	46.88	47.32	50.51	67.20	53.52	66.75	51.33	12.56	45.85	47.05	44.49	54.81	46.81	46.89	53.60	49.42	64.77	65.70
TiO_2	0.01	0.05	0.00	0.10	0.07	0.06	0.06	0.66	0.01	0.17	0.09	0.00	0.05	0.35	0.31	0.07	0.03	0.01	0.00
Al_2O_3	0.76	3.46	4.82	0.48	21.02	28.60	18.42	2.41	0.69	4.57	4.60	3.88	28.06	4.72	4.72	5.89	5.99	17.52	17.55
CaO	1.38	1.41	1.51	11.43	2.06	12.25	2.69	16.24	0.25	2.42	1.51	1.57	12.11	2.10	2.47	0.49	1.19	0.02	0.04
Na_2O	0.76	0.39	0.43	7.14	8.90	4.75	8.70	0.18	1.53	0.61	1.66	1.51	4.83	0.22	0.37	0.01	0.20	0.55	2.21
K_2O	0.37	0.21	0.46	0.05	0.25	0.03	0.85	0.05	0.27	1.14	0.36	1.84	0.01	**0.26**	0.50	9.47	8.66	16.91	14.42
FeO	28.44	23.46	22.56	27.20	1.85	0.99	1.58	11.00	62.88	27.32	21.07	26.80	0.99	20.64	21.69	13.02	11.93	0.02	0.08
MgO	11.55	13.26	14.05	2.66	0.08	0.24	0.26	16.88	1.27	9.58	14.37	8.74	0.14	13.67	11.68	7.80	7.53	0.02	0.00
MnO	0.08	0.03	0.00	0.67	0.09	0.00	0.00	0.30	0.05	0.05	0.04	0.00	0.00	0.08	0.00	0.00	0.05	0.00	0.09
P_2O_5	0.00	0.01	0.00	0.00	0.00	0.05	0.25	0.00	0.08	0.00	0.04	0.05	0.08	0.00	0.01	0.02	0.00	0.00	0.04
Cl	na	na	0.00	na	0.00	0.00	0.00	na	0.04	na	0.00	0.00	0.00	na	na	0.07	0.11	0.00	0.00
F	na	na	na	na	na	na	na	na	0.00	na	0.12	na	na	na	na	na	na	na	na
ZnO	na	na	0.11	na	0.00	0.03	0.00	na	na	na	na	0.00	0.00	na	na	0.08	0.00	0.00	0.00
Cr_2O_3	0.00	0.00	na	na	na	na	na	na	0.00	0.00	0.00	na	na	0.00	0.02	0.00	0.00	0.00	0.04
Total	87.24	89.18	91.27	100.23	101.52	100.52	99.57	99.06	79.63	91.71	90.93	88.88	101.09	88.84	88.67	90.55	85.11	99.84	100.19
An					11	59	14						58					0	0
Ab					87	41	81						42					5	19
Or					2	0	5						0					95	81

[a] Compositions of some primary minerals are given for comparison. Abbreviations: vn, vein; inn halo, inner halo; host-R, host rock; bckgrd, background; fac, facies; brw, brown; gr, green; dk, dark; phyll, phyllosilicate; cpx, clinopyroxene; sec F, secondary feldspar; mag, magmatic; ox/phyll, iron oxyhydroxide/phyllosilicate mixture; pl, plagioclase; sm, smectite; cel, celadonite; sec KF, secondary potassic feldspar; or, orange; brwish, brownish; c, colorless; be, beige; rep, replacing; cent, center; hydgt, hydrogarnet; ves, vesicle; fr, fresh; An, anorthite; Ab, albite; Or, orthose; na, not analyzed.

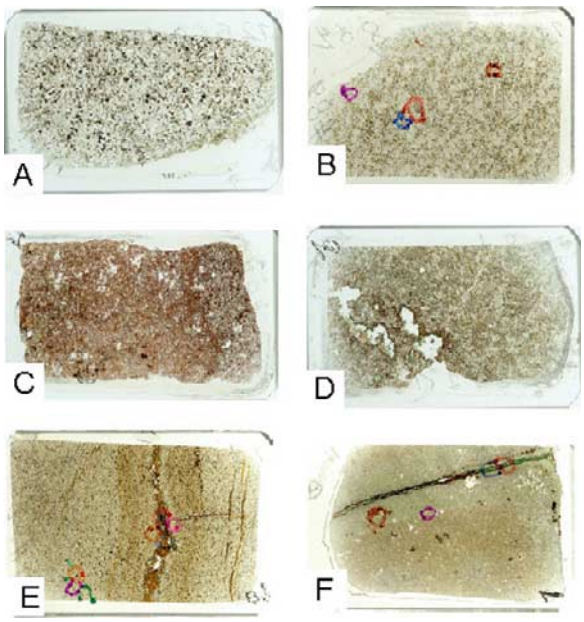

Figure 2. General view of thin sections representative of the various alteration types of this study. Plane polarized light. Length and width of each thin section are 4.5 and 3 cm, respectively. The various brightly colored circles correspond to the zones analyzed by electron microprobe. (a) Sample 206-1256D-11R-4, 67–71 cm. Coarse grained basalt from the lava pond presenting the background alteration. (b) Sample 206-1256D-12R-8, 62–68 cm. Medium grained basalt from the bottom of the lava pond presenting the background alteration. (c) Sample 206-1256D-57R-3, 15–19 cm. Red hydrothermal facies. The red color of this medium grained basalt is due to abundant iron-oxyhydroxides. (d) Sample 206-1256D-57R-2, 128–131 cm. Green hydrothermal facies. The green color of this medium grained basalt is due to abundant celadonites. Large vugs are filled with minor celadonite (dark green) at the rim and silica-minerals (colorless) at the center. (e) Sample 206-1256D-26R-6, 18–21 cm. Fine grained basalt crosscut by a brown phyllosilicate vein. Note the brown alteration halo adjacent to this vein and the general brownish staining of the whole thin section. (f) Sample 206-1256D-67R-1, 47–50 cm. Fine grained basalt crosscut by a dark orange-brown iron oxyhydroxide and dark green celadonite vein. Note the adjacent dark green alteration halo and the brown host rock.

filling vesicles and pore spaces. These secondary minerals constitute ~12% of the halo. Further from the halo, host rock shows no orange-brown staining. Orange-brown material (Table 2), here associated with quartz in vesicles and pore spaces is less abundant and some pyrite occurs. Secondary minerals represent ~8% of the host rock. We propose that, similarly to secondary green clinopyroxene mentioned in some coarse grained massive units from Hole 504B [*Laverne*, 1983, 1993; *Vanko et al.*, 1996] and in the lava pond from Hole 1256D [*Shipboard Scientific Party*, 2003; *Laverne*, 2005], this secondary green Fe-Na enriched clinopyroxene has a deuteric origin. Textural evidences suggest the same origin for albite, although deuteric albite has never been reported in oceanic crust. Nevertheless, this point requires further studies. Brown or orange halos of the sample 206-1256D-26R-6, 18–21 cm formed later than deuteric alteration. This type of alteration halo is commonly interpreted as due to halmyrolysis, i.e., basalt-seawater interaction under oxidizing conditions with high water/rock ratio [e.g., *Honnorez*, 1981; *Alt et al.*, 1996; *Laverne et al.*, 1996]. Secondary green Na-rich clinopyroxene and albite probably have a deutric origin, but this point needs further study. The three various parts of sample 206-1256D-26R-6, 18–21 cm (i.e., vein, brown halo, adjacent host rock) have been carefully separated and analyzed for the N isotopes study. Sample 206-1256D-67R-1, 47–50 cm (Figure 2f) displays a 1 mm thick dark green vein, composed of dark orange-brown iron oxyhydroxide at the edge and dark green celadonite + very small isolated globules of colorless silica-minerals at the center (Table 2). The adjacent dark green alteration halo is 5–6 mm thick. In its innermost part (1 mm thick), celadonite extensively replaces small clinopyroxene crystals composing, with plagioclase, the plumose texture mesostasis, whereas in its outermost part, celadonite occurs in the interplumose areas, and, when associated with silica-minerals globules and Ti-rich hydrogarnet (Table 2) [*Laverne*, 2005], completely replaces olivine and fills vesicles. Plagioclase phenocrysts are completely replaced by brownish smectite (Table 2). The host rock adjacent to the dark green halo is slightly brown, due to pale brown staining of the plumose texture groundmass. Vesicles and pore spaces are filled with silica-mineral and orange brown phyllosilicate, but neither celadonite nor hydrogarnet. Plagioclase phenocrysts are replaced by brownish phyllosilicate at the core and albite at the rim (Table 2). Both dark green halo and brown adjacent rock contain ~8% of secondary minerals. The celadonite-rich dark green halos or black halos are frequent in young oceanic basalts and are interpreted as reflecting interaction with a mixture of low-T hydrothermal fluids enriched in iron, silica and alkalis, and seawater [*Honnorez*, 1981; *Alt and Honnorez*, 1984; *Alt et al.*, 1986; *Buatier and Honnorez*, 1990; *Laverne*, 1993; *Belarouchi et al.*, 1996; *Alt*, 1999, 2004]. The whole sample 206-1256D-67R-1, 47–50 cm is likely a mixed

halo, whose internal dark green part would have formed by low-T hydrothermal alteration, and the external brownish part, formed later by halmyrolisis. The three various parts of this sample (vein, dark green halo, brown host rock) have been separated and analyzed for N isotopes.

[10] In order to compare the general background alteration to more specific and localized types of alteration, two basalt samples have been selected from a unique 41 cm long interval at 648.06 mbsf exhibiting spectacular brick-red (sample 206-1256D-57R-3, 15–19 cm for N study (Figure 2c), and sample 206-1256D-57R-3, 5–8 cm for microprobe study) and blue-green (sample 206-1256D-57R-2, 118–127 cm for N study (Figure 2d), and sample 206-1256D-57R-3, 0–1 cm for microprobe study) colors. These basalts are extensively altered (80–90%). Thin section observation of the brick-red facies shows that the color is due to the great abundance of iron oxyhydroxides (Table 2), filling large vugs, replacing magmatic clinopyroxene and composing numerous veinlets. In this sample, olivine is completely replaced by celadonite + Si-mineral ± Ca-carbonate, and plagioclase is partly or completely replaced by K-feldspar (Or_{81-99}; Table 2) and crosscut by numerous iron oxyhydroxides veinlets. Thin section examination of the blue-green facies shows that the color results from the great abundance of celadonite (Table 2), completely replacing olivine and filling pore spaces. Clinopyroxene is extensively replaced by colorless or "dusty" fibers of saponite ± celadonite. Vugs are composed, from the rim to the center, of a thin layer of iron oxyhydroxides, colorless saponite, celadonite, and quartz or Ca-carbonate in the largest vugs. Bulk-rock chemical analyses carried out during Leg 206 indicate that this interval is enriched in K, P, Fe and Mn, and depleted in Mg and Ca compared with background alteration basalts. Both brick-red and blue-green facies samples are interpreted as resulting from intense low-T alteration [*Shipboard Scientific Party*, 2003].

4. Analytical Procedures

[11] Electron microprobe analyses of primary and secondary minerals were carried out at two places: (1) runs B1 to B6 at IFREMER (Brest, France) on a Cameca SX50 with correction program ZAF [*Pouchou and Pichoir*, 1985]. Operating conditions were: 15 kV accelerating voltage, 15 nA specimen current, 1 μm spot size, 6 s counting time; and (2) runs P1 to P3 at Paris VII University on a SX50 (runs P1 and P2) and SX100 (run P3). Operating conditions were: 15 kV accelerating voltage, 10 nA specimen current, 10 μm spot size, 10 s counting time. The precision of the methods used is better than 0.5% for the measured concentrations.

[12] Nitrogen extraction was performed using combustion of the samples in tubes sealed under vacuum [*Boyd et al.*, 1994; *Busigny et al.*, 2005]. The whole-rock samples were ground to thin powders and homogenized. Grains size was mostly between 32 and 63 μm. For three samples (206-1256D-16R-1, 88–95 cm; 206-1256D-32R-1, 114–120 cm; 206-1256D-52R-1, 8–15 cm), half of the powder was leached with deionized water at neutral pH and room temperature before combustion. Results obtained from combustion on both leached and unleached powders were compared in order to test if N occurred, at least partially, as exchangeable chemical species. Although the technique used for N content and $\delta^{15}N$ determinations has been thoroughly described elsewhere [*Busigny et al.*, 2005], details relevant to the present work are recalled herein.

[13] Samples powders (2.7 to 58.2 mg) were embedded in platinum foils and loaded with purified CuO, Cu and CaO in quartz glass tubes connected to a vacuum line. They were degassed at 450°C during 12 hr under vacuum to avoid contamination by atmospheric N. The line was isolated from the pumps and saturated with O_2 pressure generated with CuO heated to 900°C for 1 hr, allowing removal of all organic contamination and potential residual adsorbed atmospheric N of the samples. O_2 was then re-adsorbed by cooling the CuO to 450°C and the line was evacuated. At pressure $< 10^{-6}$ Torr, the tubes were sealed to give evacuated ampoules. Ampoules were heated in a muffle furnace at 950 or 1050°C for 6 hr followed by a step at 600°C for 2 hr. This heating allowed (1) sample combustion under oxygen pressure at 950 or 1050°C, (2) nitrous oxide reduction by copper, and (3) trapping of carbon dioxide by CaO at 600°C. It can be noted that duplicate analyses of most samples were performed using combustion temperatures of both 950 and 1050°C in order to make sure that N had been efficiently extracted at 950°C.

[14] Ampoules were loaded into a vacuum line and opened with a tube cracker. Nitrogen was purified and quantified as dinitrogen N_2 by capacitance manometry with a precision better than 8% (2σ). The gas was then isotopically analyzed using a

Table 3. Results of N Analyses of Samples From Site 1256[a]

Hole	Core Section	Interval, cm	Depth, mbsf	Rock Type	T°, °C	Weight, mg	N, nmol	N, ppm	δ^{15}N, ‰
1256C	4R-1	13–20	245.13	chert	950	25.59	19	9.9	3.1
					1050	28.16	20	9.7	3.0
								9.8	3.1
1256C	8R-1	101–108	276.51	bckgrd alt.	950	35.67	7	2.3	5.6
					1050	58.21	11	2.5	6.0
								2.4	5.8
1256D	9R-4	90–97	327.27	bckgrd alt.	950	39.68	9	3.1	5.7
					1050	53.22	13	3.3	5.9
								3.2	5.8
1256D	12R-8	71–79	351.21	bckgrd alt.	950	55.27	9	2.0	3.9
					1050	49.13	9	2.3	3.9
								2.1	3.9
1256D	16R-1	88–95	369.78	bckgrd alt.	950	45.24	9	2.7	4.4
					1050	40.88	9	2.8	3.3
				*	1050	49.75	11	3.0	3.3
								2.8	3.7
1256D	22R-2	120–127	408.43	bckgrd alt.	1050	51.52	8	2.0	4.3
1256D	24R-1	132–139	420.82	bckgrd alt.	950	43	10	3.1	4.1
					1050	46.73	11	3.2	n.d.
					1050	39.39	8	2.7	3.0
								3.0	3.6
1256D	26R-6	18–21	445.49	host rock	1050	53.85	15	3.9	9.1
				halo	1050	51.86	21	5.6	9.1
				vein	1050	14.46	356	344	0.4
				vein	1050	2.73	72	365	0.4
								354	0.4
1256D	27R-1	130–137	446.70	bckgrd alt.	950	48.38	11	2.9	2.7
					1050	38.41	10	3.4	3.3
								3.2	3.0
1256D	32R-1	114–120	476.34	bckgrd alt.	950	50.42	13	3.6	4.8
					1050	50.08	11	2.9	4.8
				*	1050	53.19	13	3.2	5.0
								3.2	4.9
1256D	37R-1	36–43	500.46	bckgrd alt.	1050	52.02	7	1.8	2.8
1256D	41R-2	26–23	526.26	bckgrd alt.	950	50.81	11	2.8	4.2
					1050	43.72	9	2.6	3.7
								2.7	3.9
1256D	47R-2	121–126	573.71	bckgrd alt.	1050	44.59	11	3.1	3.6
1256D	52R-1	8–15	600.78	bckgrd alt.	950	55.03	13	3.1	5.2
					1050	37.59	11	3.9	4.7
				*	1050	45.59	11	3.2	5.1
								3.4	5.0
1256D	57R-2	118–127	648.02	green facies	1050	31.78	24	10.2	−2.6
					1050	29.56	20	9.3	−2.8
								9.7	−2.7
1256D	57R-3	15–19	648.29	red facies	1050	31.39	20	8.6	−3.8
1256D	57R-4	118–125	650.83	bckgrd alt.	950	49.14	15	4.0	3.6
					1050	54.8	19	4.6	3.2
								4.3	3.4
1256D	67R-1	47–50	715.27	host rock	1050	39.27	17	5.9	6.1
				halo	1050	40.74	17	5.7	6.9
				vein	1050	5.79	204	491	−2.1
1256D	69R-1	24–33	724.34	bckgrd alt.	1050	57	16	3.8	2.6
1256D	74R-2	102–111	749.56	bckgrd alt.	950	43.83	5	1.3	1.5
					1050	49.92	6	1.5	1.6
								1.4	1.6
BAS-206				composite	1050	52.43	7	1.6	2.1

[a] Depth of sampling given in meters below seafloor (mbsf); T°, temperature of N extraction; Weight, sample weight; N (nmol), amount of N extracted. The precisions on nitrogen content and δ^{15}N are better than 8% and 0.5‰, respectively. The asterisks indicate the three samples previously leached in deionized water.

triple-collector static mass spectrometer. Variations in the N isotopic composition of the samples are expressed in the usual δ notation (‰): $\delta^{15}N_{sample}$ (‰) = $[(^{15}N/^{14}N)_{sample}/(^{15}N/^{14}N)_{standard} - 1] \times 1000$, where the standard is atmospheric N_2. Possible carbon monoxide and atmospheric contamination was monitored in the mass spectrometer using m/z = 12, 30 and 40 (Ar). The $\delta^{15}N$ was measured with an accuracy of ±0.5‰ (2σ), estimated from the reproducibility of international standards (IAEA-N1 and -N2). The nitrogen blank has been evaluated by analyzing several sealed tubes (n = 40) prepared as described above but without sample powder. The blank amount is comprised between 0.39 and 0.95 nmol N, with mean value at 0.65 ± 0.30 nmol (2σ). The blank $\delta^{15}N$ values vary from −6.4 to −0.8‰, and define a Gaussian distribution with a mean value at −3.7 ± 2.7‰ (2σ; for more details, see *Busigny et al.* [2005]). A blank correction was applied to each sample measurement. The amount of N extracted from samples ranged from 5 to 356 nmol (Table 3), implying that the blank was <15% of the total N amount.

5. Results

[15] Nitrogen content and isotopic composition of the samples from Site 1256 are reported in Table 3. N contents and $\delta^{15}N$ values vary over large ranges from 1.4 to 491 ppm and −3.8 to +9.1‰, respectively. Table 3 shows that analytical reproducibility is very good. Notably, each sample displays identical results for both combustions at 950 and 1050°C. This suggests that N was efficiently extracted by sealed tube combustion at temperature higher than 950°C. However, the possible occurrence of strongly refractory N-bearing phase cannot be totally ruled out.

[16] The three samples leached with deionized water before N extraction show N content and $\delta^{15}N$ indistinguishable from their unleached counterparts. This observation indicates that N occurs neither as water-soluble phase like salts (such as NH_4Cl) nor as exchangeable chemical species.

[17] Background alteration samples show moderately low N contents (between 1.4 and 4.3 ppm) that are however higher than fresh degassed MORB (∼1.1 ppm [*Sakai et al.*, 1984; *Exley et al.*, 1987; *Marty et al.*, 1995]). Their $\delta^{15}N$ values vary over a large range from +1.6 to +5.8‰ (Table 3). Nitrogen content and $\delta^{15}N$ value of the chert are 9.8 ppm and +3.1‰, respectively. These values compare well with the range previously determined for cherts of various localities [*Sano and Pillinger*, 1990; *Pinti et al.*, 2001], for which estimates of N contents and $\delta^{15}N$ vary from 0.27 to 15 ppm and −3.8 to +9.9‰, respectively. Veins, alteration halos and host rocks separated from two samples show significant enrichment in N relative to background alteration basalts. Sample 206-1256D-26R-6, 18–21 cm displays identical $\delta^{15}N$ value in host rock and alteration halo (+9.1‰). In contrast, its N content is higher in the halo (5.6 ppm) than in the host rock (3.9 ppm). Sample 206-1256D-67R-1, 47–50 cm show similar N contents and $\delta^{15}N$ values in host rock and alteration halo, being ∼5.8 ppm and ∼+6.5‰, respectively. Veins of both samples show remarkably high N contents (354 and 491 ppm) associated with slightly low $\delta^{15}N$ values (+0.4 and −2.1‰). Red and green facies samples display high N contents (8.6 and 9.7 ppm, respectively) and negative $\delta^{15}N$ (−3.8 and −2.7‰).

[18] Figure 3 illustrates downhole variations of N content and $\delta^{15}N$ value of samples from Site 1256. Nitrogen content of background alteration samples does not show any specific variation with depth (Figure 3a). It varies monotonically downhole except between 600 and 725 mbsf where N content tends to increase slightly. This 125 m depth interval includes the green and red facies samples that are both characterized by high N content and represent a higher extent of alteration (80–90% of secondary minerals) than other sections of the hole [*Shipboard Scientific Party*, 2003]. Contrasting with N content variation, N isotopic composition is not monotonous downhole. Background alteration samples show a rough decrease of $\delta^{15}N$ with increasing depth. This decrease ranges from +5.8‰ at the top of the section to +1.6‰ at the bottom (Figure 3b). This rough trend is bracketed by veins and halos/host rocks $\delta^{15}N$ values (Figure 3b). Strikingly, N isotopic fractionation between veins and halos/host rocks ($\Delta^{15}N_{halo\text{-}vein} = \delta^{15}N_{halo} - \delta^{15}N_{vein}$) is similar for the two samples for which veins were separated and averages ∼9‰.

6. Discussion

6.1. Nitrogen Speciation in Altered Oceanic Basalts

[19] The determination of N speciation in altered oceanic basalt is not straightforward. In samples from Site 1256, nitrogen analyses of mineral separates were not performed because of the very

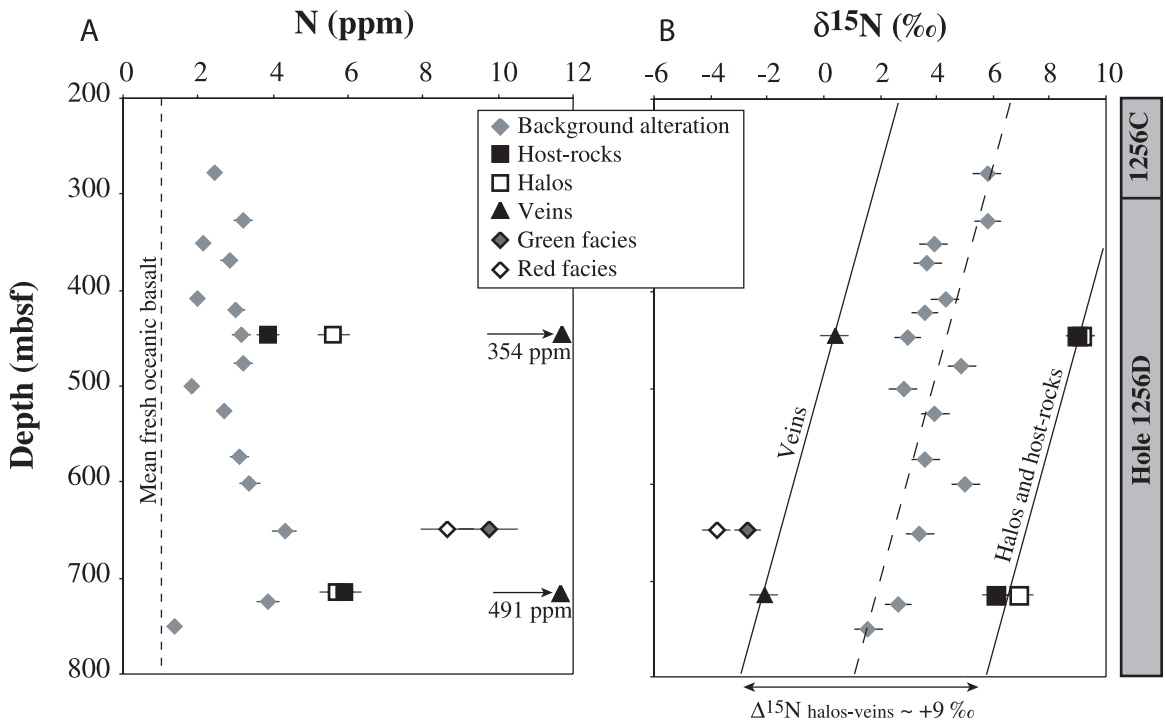

Figure 3. Downhole variations of (a) nitrogen concentration and (b) isotopic composition in basalts from ODP Site 1256, Leg 206 (only average values are plotted). Six types of samples are distinguished: (1) background alteration samples, (2) veins, (3) alteration halos related to veins, (4) host rocks adjacent to alteration halos, (5) celadonite-rich hydrothermal green facies, and (6) iron oxyhydroxides (and celadonite) rich hydrothermal red facies. Dotted line in Figure 3a represents mean fresh oceanic basalts N content calculated from previous data [*Sakai et al.*, 1984; *Exley et al.*, 1987; *Marty et al.*, 1995].

small size of minerals. The analysis of N content using in-situ techniques such as infrared spectroscopy was not attempted due to the high limit of N detection. Nevertheless, several inferences can be deduced from the results of the present work. First, N extracted from the samples is not derived from organic molecules because samples were heated at 450°C under an O_2 atmosphere during 1 hr, allowing removal of any organic matter by combustion. Second, N is not present as an ammonium salt (e.g., NH_4Cl, $[NH_4]_2SO_4$) because N contents in leached samples are similar to their unleached counterparts (Table 3). Finally, N more likely occurs structurally bound in minerals since the samples were analyzed as fine powders (<63 μm) degassed under vacuum at 450°C during 12 hr.

[20] In crustal rocks, N fixed in minerals usually occurs as ammonium ion, NH_4^+ [e.g., *Vedder*, 1964, 1965]. Nitrogen is substituting either for (1) potassium in K-bearing minerals such as K-feldspar and micas or for (2) Na-Ca in minerals such as plagioclase [e.g., *Honma and Itihara*, 1981]. Samples from Site 1256 showing the highest N content contain K-bearing mineral (celadonite ± K-feldspar). This is particularly striking for the green and red facies, both containing celadonite and K-feldspar. The high N content in the vein of sample 206-1256D-67R-1, 47–50 cm is clearly related to its very K-rich celadonitic composition (up to 8.3 wt% K_2O). The associated dark green halo is also rich in celadonite, explaining its relatively high nitrogen content (5.7 ppm). In the adjacent orange basalt, the occurrence of albite partly replacing plagioclase phenocrysts could explain the high nitrogen content (5.9 ppm).

[21] Sample 206-1256D-26R-6, 18–21 cm contains neither celadonite nor secondary K-feldspar. The occurrence of secondary green clinopyroxene strongly enriched in Na with respect to primary clinopyroxene and partial albitization of feldspar in the inner part of the brown alteration halo could explain the high N content of the vein. Orange phyllosilicate and/or iron oxyhydroxides contain some K_2O (up to 1.14 wt%; Table 2) and may thus bear ammonium. They are less abundant in the host rock than in the orange halo, possibly explaining its lower N content (3.9 ppm instead of 5.6 ppm). It should be noted that N content of the host rock is in

the highest range of the background alteration samples.

[22] The studied background alteration samples do not contain obvious NH_4-bearing minerals such as celadonite and secondary K- or Na-feldspars. However smectite, the main secondary mineral of these basalts, always contain small amounts of K_2O (up to 1 wt%, see for instance sample 206-1256D-34R-4, 37–40 cm in Table 2). It is thus suggested that smectite may incorporate a quantity of NH_4 sufficient to account for the slight increase in N content with respect to fresh MORB. This inference is supported by previous NH_4 occurrence in smectites of various sedimentary environments [*Chourabi and Fripiat*, 1981; *Lindgreen*, 1994; *Pironon et al.*, 2003].

6.2. Nitrogen Enrichment During Alteration of Oceanic Basalts

[23] The two veins separated from Site 1256 basalts show particularly high N content of 354 and 491 ppm, respectively. These high concentrations indicate that N was strongly enriched in the circulating fluids. Nitrogen enrichment in fluids implies either N addition to oceanic crust by fluids or, on the contrary, N leaching from the crust to fluids. Several lines of evidence suggest that basalts from Site 1256 were enriched in N during their alteration. A first evidence is provided by comparing samples from Site 1256 with fresh MORB (Figure 3a). Nitrogen content of background alteration samples from Site 1256 ranges between 1.4 and 4.3 ppm and averages 2.8 ppm. In contrast, fresh degassed MORB from various worldwide localities (Atlantic, Pacific and Indian oceans) show N content ranging from 0.3 to 2.8 ppm, with an average value of 1.1 ppm [*Sakai et al.*, 1984; *Exley et al.*, 1987; *Marty et al.*, 1995]. Although samples from Site 1256 overlap MOR basalts, they show a significant N enrichment that can be assigned to alteration process (Figure 3a). A second evidence arises from the comparison of alteration halos and related host rocks with background alteration samples. Because alteration halos and host rocks are much more affected by low-T alteration than background alteration samples, their sensitive N enrichment (~5.3 ppm for host rocks and halos compared to ~2.8 ppm for background samples) demonstrates that intensive interaction of basalts with circulating fluid increased their N contents. A similar comparison can be made with the green and red facies, having the most significant proportions of secondary minerals. These samples are considerably enriched in N (~9.2 ppm) compared to background alteration samples (~2.8 ppm), supporting that N is enriched during alteration process. This conclusion contrasts with results of a previous study on the Hole 504B altered basalts [*Erzinger and Bach*, 1996], where N content was found either unchanged or decreased during alteration process at low and high temperature. *Erzinger and Bach* [1996] interpreted the loss of N as a result of leaching process, by analogy with downhole variations observed for Zn concentrations. Because the leaching of Zn occurs at high temperature > 350°C [e.g., *Alt et al.*, 1996] and the temperature of alteration at Site 1256 is typically ~100°C (J. C. Alt et al. et al., Spreading rate dependence of upper ocean crust alteration: A study of crust formed by superfast spreading in the eastern Pacific, manuscript in preparation, 2005; hereinafter referred to as Alt et al., manuscript in preparation, 2005), the two different behaviors of N may arise from different types of alteration processes. Alternatively, it could originate from analytical discrepancies between the pyrolysis technique used by *Erzinger and Bach* [1996] and our sealed-tube combustion technique. Notably, Erzinger and Bach heated their samples in molybdenum crucible although it has been shown that nitrogen can be adsorbed by molybdenum even at high temperature [*Fromm and Jehn*, 1968; *Martinz and Prandini*, 1994; *Yokochi*, 2005]. The low N concentration measured in Hole 504B altered basalts may thus result from an incomplete recovery of nitrogen. Further analysis of these samples by sealed tube combustion would permit to test this hypothesis.

[24] Interestingly, the conclusion that N is enriched during alteration of basaltic rocks has been suggested once in a previous study of spilitized basalts from the Cornubian massif, Southwest England [*Hall*, 1989]. In this work, concentrations of fixed, exchangeable and total NH_4 were determined using a colorimetric method. Total NH_4 concentrations of spilitized basalts showed values up to 182 ppm, and averaged 54 ppm. Most of the NH_4 was fixed in minerals (~50 ppm on average) while a low proportion was exchangeable (~5 ppm). Fixed NH_4 occurred mainly in secondary minerals such as micas and feldspars [*Hall*, 1989]. Exchangeable NH_4 was suggested to be concentrated in sepiolite, i.e., a zeolite. Although it remains unknown if spilitic alteration of Cornubian basalts can be considered as representative of oceanic crust alteration, these data illustrate that alteration processes can produce significant N enrichment in mafic

rocks, in good agreement with the present results on samples from Site 1256.

6.3. Source and Speciation of N in Hydrothermal Fluid

[25] Considering that N is enriched during alteration of oceanic crust, it is essential to discuss the speciation and origin of N provided to the crust. This can be addressed using N isotope data. Temperatures of alteration of samples from Site 1256 have been shown to vary in a small range, between 70 and 100°C, determined from oxygen isotope fractionations (Alt et al., manuscript in preparation, 2005). Because of this small temperature range, N isotope fractionation during fluid-rock interaction is expected to be approximately constant if the speciation of N in both rock and fluid remains unchanged. Assuming that each vein represents a part of the hydrothermal fluid, that was trap and precipitated, the striking constancy of N isotope fractionation between veins and associated halos/host rocks $\Delta^{15}N_{halo\text{-}vein}$($\Delta^{15}N_{halo\text{-}vein} = \delta^{15}N_{halo} - \delta^{15}N_{vein} \sim +9‰$; see Figure 3b) supports that isotopic equilibrium was reached. In this scenario, each vein would record the composition of the fluid at a certain depth. If N is considered to occur as fixed NH_4 in altered basalts (see discussion above), the constant $\Delta^{15}N_{halo\text{-}vein}$ can be used to constrain N speciation in hydrothermal fluids. Nitrogen in hydrothermal fluid could occur as dissolved NH_4^+, NH_3 or N_2. The hypothesis of NH_4 dissolved in fluid can be easily rejected as exchange between $(NH_4)_{fluid}$ and $(NH_4)_{rock}$ is not expected to induce any N isotopes fractionation $\Delta^{15}N_{rock\text{-}fluid}$ (i.e., $\Delta^{15}N_{rock\text{-}fluid} = \delta^{15}N_{rock} - \delta^{15}N_{fluid} \sim 0‰$). The hypothesis that N occurs in fluid as NH_3 or N_2 can be tested by comparing theoretical and measured N isotopes fractionations. Theoretical isotopes fractionation factors among various chemical species in the N system were determined by *Hanschmann* [1981]. On the basis of an interpolation of the data of *Hanschmann* [1981], the calculated $\Delta^{15}N_{rock\text{-}fluid}$ would range from +26.8 to +23.8‰ at temperature of 70–100°C for an isotopic exchange reaction between NH_4 and NH_3. The same calculation for an exchange reaction between NH_4 and N_2 would provide a $\Delta^{15}N_{rock\text{-}fluid}$ ranging from +9.6 to +8.4‰ in the same temperature range. This last value is consistent with observed $\Delta^{15}N_{halo\text{-}vein}$ of ∼+9‰, suggesting that (1) N in hydrothermal fluids may have been carried as N_2 rather than NH_3 and (2) N in altered halos and host rocks occurred as NH_4^+, in good agreement with inference from petrological observations. The occurrence of N_2 as the main N species in hydrothermal fluid should be tested in future works, analyzing specifically fluid inclusions supposed to represent primary trapped fluid.

[26] Two main sources can provide N_2 to fluids infiltrating through the crust. The first would derive directly from deep seawater, for which N_2 is the major dissolved N species (0.59 mM [*Charlou et al.*, 2000]). The second source would correspond to mantle N either (1) degassed from magmas rising up to the surface and mixed with hydrothermal fluid or (2) leached from oceanic crust during fluid circulation. In the following section, two possible scenarios are explored in order to explain the variations of N isotopes in samples from Site 1256: "case 1" assumes deep seawater as a unique source of N_2, and "case 2" considers that N_2 originates from a mixing of deep seawater with magmatic gases.

[27] In case 1, the rough $\delta^{15}N$ decrease from top to bottom of the Leg 206 section (Figure 3b) may indicate an evolution of seawater-derived fluid circulating through the crust. This could reflect an interaction of the fluid with host rocks, through successive uptake of N from the fluid to basalts, followed by N isotopic equilibration. Assuming that N occurs as N_2 in the fluid and is progressively fixed as NH_4^+ in basalts, the effect of N loss from the fluid on its stable isotope composition can be modeled as Rayleigh distillation. Each small aliquot of NH_4 produced from N_2 remains trapped in the host basalt while the fluid continues flowing through the crust. The Rayleigh distillation describes an exponential enrichment in the residual fluid that is calculated as

$$\delta^{15}N = \delta^{15}N_0 - 1000\left(F^{(\alpha-1)} - 1\right), \qquad (1)$$

where $\delta^{15}N_0$ and $\delta^{15}N$ are the isotopic composition of the fluid before and after N loss to the basalt, F is the N fraction remaining in the fluid after the loss and α is the fractionation factor between N_2 in the fluid and NH_4 fixed in the basalt. The fractionation factor α can be interpolated from values given by *Hanschmann* [1981]. Figure 4a shows that N isotopes fractionation between N_2 of the fluid and NH_4 fixed in basalts produce a decrease of $\delta^{15}N$ value in the remaining fluid. Indeed, NH_4^+ is known to be enriched in ^{15}N relative to N_2 (e.g., *Haendel et al.*, 1986; *Bebout and Fogel*, 1992] and N isotopic fractionation $\Delta^{15}N_{rock\text{-}fluid}$ between NH_4^+ and N_2 is very large at low temperature of 70–100°C (∼+9‰ [*Hanschmann*, 1981]). Figure 4a

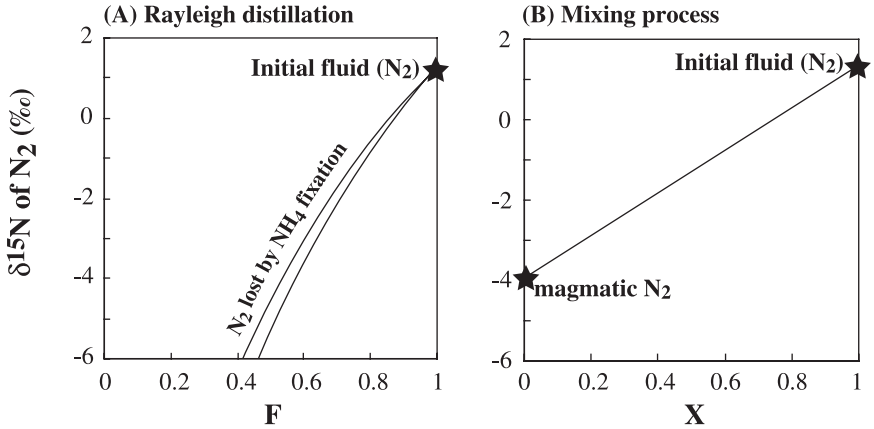

Figure 4. Evolution of N_2 isotopic composition of hydrothermal fluid for the two models described in the main text. (a) Rayleigh distillation for an exchange between N_2(fluid) and NH_4(mineral). The two curves represent calculations for temperatures of 70 and 100°C, using fractionation factors of 0.9905 and 0.9916, respectively [from *Hanschmann*, 1981]. $\delta^{15}N$ of the fluid is plotted versus the fraction (F) of N remaining in the fluid. $\delta^{15}N_0$ was assumed at +1.3‰ for the initial fluid as deduced from linear extrapolation of the veins $\delta^{15}N$ (assumed to represent the fluid) at a depth of 250 m corresponding to the sediment-basalt boundary (Figure 3b). (b) Mixing model between an initial fluid and a magmatic N_2 from basalt vesicles. $\delta^{15}N$ of the fluid resulting from mixing is plotted versus N fraction of the initial fluid (X). $\delta^{15}N_0$ of the initial fluid is assumed at +1.3‰, and $\delta^{15}N_{magmatic}$ is assumed at −4‰ (from data on fresh MORB vesicles [*Javoy and Pineau*, 1991; *Marty and Humbert*, 1997; *Marty and Zimmermann*, 1999; *Nishio et al.*, 1999; *Cartigny et al.*, 2001]).

shows that $\delta^{15}N$ of the remaining fluid decreases from +1.3 to −4.0‰ when approximately 50% of N is lost (i.e., F = 0.5). Unfortunately, the proportion of N lost from the fluid to the rock cannot be determined from available data on samples from Site 1256 since N concentration in the fluid depends not only on N loss but also on the concentrations of other components, which probably varied owing to fluid-rock interaction. Although quantitative modeling cannot be derived, the low water/rock ratio characterizing alteration of samples from Site 1256 [*Shipboard Scientific Party*, 2003] may have induced strong modifications of the fluid $\delta^{15}N$ through successive loss and isotopic exchange with basalts. Rayleigh distillation process may thus be suitable to produce important variation of $\delta^{15}N$ with depth. Following this hypothesis, the progressive decrease of $\delta^{15}N$ with depth (Figure 3b) would imply that fluid flux migrated downward through the Leg 206 section. It should be noted that the formation of NH_4 from N_2 is a viable process in oceanic hydrothermalism. This is not a simple one-step reaction but can be proceed in two steps, such as,

$$N_2 + 3H_2 \Rightarrow 2NH_3, \quad (2)$$

where a reaction between nitrogen and hydrogen produces two ammonia molecules. The reality may be more complex with the hydrogen being bound in water. At moderate temperature (<250°C), the Gibbs free energy (ΔG) of reaction (2) is negative, being −16.667 and −5.941 kJ/mol at 25 and 121.85°C, respectively [*Chase*, 1998]. Therefore ammonia may be spontaneously produced at temperature of alteration of samples from Site 1256 (i.e., 70–100°C (Alt et al., manuscript in preparation, 2005)). Reaction (2) can then be followed by

$$NH_3 + H^+ \Rightarrow NH_4^+, \quad (3)$$

where ammonia reacts with a proton to produce ammonium ion. Proton can be provided by water autoionization through minerals hydroxylation related to alteration process. The constant of dissociation (pKa) of the ammonium ion in reaction (3) has been estimated at 7.928 ± 0.005 for a temperature of 75°C [*Olofsson*, 1975]. Considering temperature as constant, equilibrium of reaction (3) is mostly pH-dependent and can be written as

$$pH(75^\circ C) = 7.928 + \log\left\{\frac{[NH_3]}{[NH_4]}\right\}. \quad (4)$$

At pH 7.928, the two species (NH_4 and NH_3) will be in equal proportions and NH_3 will be dominant only for alkaline environments. For pH lower than 7.9, NH_4 will become the dominant chemical species. In hydrothermal fluids, pH is

lower than seawater (i.e., 7.8) and usually ranges from 3.1 to 7.5 [e.g., *Charlou et al.*, 1996, 2000]. Accordingly, NH_4 will always be present as the major species. It seems thus realistic to consider that NH_4 can be produced from N_2 at the conditions prevailing during low-temperature seawater/rock interaction.

[28] An alternative hypothesis to explain $\delta^{15}N$ decrease with depth in samples from Site 1256 (Figure 3b) is that N in hydrothermal fluid is progressively mixed with magmatic N_2 initially trapped in basalts (case 2). Several studies demonstrated that N_2 included in fresh MORB vesicles show negative $\delta^{15}N$ value at $\sim -4‰$ [*Javoy and Pineau*, 1991; *Marty and Humbert*, 1997; *Marty and Zimmermann*, 1999; *Nishio et al.*, 1999; *Cartigny et al.*, 2001]. If the fluid flowing through the crust initially contains N_2 with slightly positive $\delta^{15}N$ value, a progressive mixing with magmatic N_2 would lower the $\delta^{15}N$ of the resulting fluid and the basalts in equilibrium with this fluid, as observed along the Leg 206 profile (Figure 3b). This hypothesis can be modeled by a simple binary mixing between initial fluid and magmatic vesicles as

$$\delta^{15}N = X.\delta^{15}N_0 + (1 - X).\delta^{15}N_{magmatic}, \quad (5)$$

where $\delta^{15}N_0$ and $\delta^{15}N$ are the isotopic composition of the fluid before and after the mixing process, X is the N fraction of the initial fluid and $\delta^{15}N_{magmatic}$ is the N isotopic composition of the magmatic vesicles. "1 − X" represents the N fraction brought by the vesicles to the fluid. Figure 4b shows that $\delta^{15}N$ of the fluid decreases when N fraction of the initial fluid decreases. This reflects a progressive dilution of initial N with magmatic N_2 of negative $\delta^{15}N$ value. A $\delta^{15}N$ value around $-4‰$ in the fluid implies that the whole N derives from magmatic vesicles. The negative $\delta^{15}N$ value of $-2.1‰$ measured in the vein from sample 206-1256D-67R-1, 47–50 cm would reflect a mixing with ~60% of magmatic N_2. This is in good agreement with previous studies suggesting that black halos originate from interaction of the basalt with low-temperature hydrothermal fluids mixed with seawater (see section 3). The very negative $\delta^{15}N$ values (-3.8 and $-2.7‰$) observed in the red and green facies samples may also reflect a very large involvement of magmatic component in hydrothermal fluid. It is worth noting that this model is slightly simplistic as $\delta^{15}N$ of magmatic N_2 trapped in basalts vesicles is likely not perfectly homogeneous at $-4‰$. Nevertheless, it illustrates that the variation of $\delta^{15}N$ in samples from Site 1256 can result from a mixing of hydrothermal fluid with magmatic gases. In this case, the decrease of $\delta^{15}N$ with increasing depth (Figure 3b) would require, once again, a fluid flux migrating downward through the crust.

[29] The two models presented above are suitable to explain $\delta^{15}N$ decrease with depth observed in Site 1256 basalts. Although it is not possible to settle between these two hypotheses from current data, a mixing of the fluid with magmatic gases contained in basalt vesicles seems to be unavoidable when hydrothermal fluid is flowing through the crust. We thus suggest that the second hypothesis is the most likely even if the first one may also involve in decreasing $\delta^{15}N$ value.

7. Conclusions

[30] Basalts from Site 1256 display a clear enrichment in N during alteration process, contrasting with previous results obtained on basalts from DSDP/ODP Hole 504B [*Erzinger and Bach*, 1996].

[31] Nitrogen of altered basalts likely occurs as NH_4^+ fixed in various secondary minerals. Celadonite, K- and Na-feldspars seem to be the main N-repositories but smectite may also incorporate a small concentration of nitrogen. Because of its presence in most basalts, smectite may represent a large proportion of N-fixed during alteration of upper oceanic crust.

[32] Nitrogen isotopic fractionation between veins and alteration halos suggests that N of hydrothermal fluid mainly occurs as N_2. A decrease of $\delta^{15}N$ with increasing depth supports that N of hydrothermal fluid is either (1) progressively isotopically fractionated during exchange with basalts and/or (2) mixed with magmatic N_2 enclosed in basalts vesicles.

Acknowledgments

[33] Ocean Drilling Program is gratefully acknowledged for providing rock samples. We thank all the petrologists and structuralists having sailed for Leg 206 for their help and fruitful discussions. Pierre Agrinier and Pierre Cartigny are greatly thanked for helpful comments. Marcel Bohn, Michel Girard, and Jean-Jacques Bourrand are thanked for their technical assistance. Jeffrey Alt and an anonymous reviewer are acknowledged for constructive comments. This study

was supported by a grant INSU TERRE - Programme 78: Groupe Oceans. Contribution IPGP 2090 and CNRS 328.

References

Alt, J. C. (1999), Very low grade hydrothermal metamorphism of basic igneous rocks, in *Very Low Grade Metamorphism*, edited by M. Frey and D. Robinson, pp. 169–201, Blackwell Sci., Malden, Mass.

Alt, J. C. (2004), Alteration of the upper oceanic crust: Mineralogy, chemistry, and processes, in *Hydrogeology of the Oceanic Lithosphere*, edited by H. Elderfield and E. Davis, pp. 456–488, Cambridge Univ. Press, New York.

Alt, J. C., and J. Honnorez (1984), Alteration of the upper oceanic crust, DSDP Site 417: Mineralogy and chemistry, *Contrib. Mineral. Petrol.*, *87*, 149–169.

Alt, J. C., J. Honnorez, C. Laverne, and R. Emmermann (1986), Hydrothermal alteration of a 1 km section through the upper oceanic crust, Deep Sea Drilling Project Hole 504B: Mineralogy, chemistry, and evolution of seawater-basalt interactions, *J. Geophys. Res.*, *91*(B10), 10,309–10,335.

Alt, J. C., D. A. H. Teagle, C. Laverne, D. Vanko, W. Bach, J. Honnorez, K. Becker, and P. A. Pezard (1996), Ridge flank alteration of upper ocean crust in the eastern Pacific: A synthesis of results for volcanic rocks of Holes 504B and 896A, *Proc. Ocean Drill. Program Sci. Results*, *148*, 435–450.

Bebout, G. E., and M. L. Fogel (1992), Nitrogen-isotope compositions of metasedimentary rocks in the Catalina Schist, California: Implications for metamorphic devolatilization history, *Geochim. Cosmochim. Acta*, *56*, 2839–2849.

Belarouchi, A., C. Laverne, P. Gente, P. Agrinier, and J. Cotten (1996), Altération à basse température des basaltes en domaine océanique et comportement des terres rares: Evidence à partir des échantillons dragués durant la mission SEADMA 1 (ride médio-atlantique, 20–24°N), *Bull. Soc. Geol. Fr.*, *167*, 543–558.

Boyd, S. R., A. Réjou-Michel, and M. Javoy (1994), Noncryogenic purification of nanomole quantities of nitrogen gas for isotopic analysis, *Anal. Chem.*, *66*, 1396–1402.

Buatier, M., and J. Honnorez (1990), Mécanismes de formation des argiles des "halos noirs" de basaltes océaniques, *C. R. Acad. Sci., Ser. II*, *310*, 1497–1503.

Busigny, V., M. Ader, and P. Cartigny (2005), Quantification and isotopic analysis of nitrogen in rocks at the ppm level using sealed-tube combustion technique: A prelude to the study of altered oceanic crust, *Chem. Geol.*, *223*, 249–259.

Cartigny, P., N. Jendrzejewski, F. Pineau, E. Petit, and M. Javoy (2001), Volatile (C, N, Ar) variability in MORB and the respective role of mantle source heterogeneity and degassing: The case of the Southwest Indian Ridge, *Earth Planet. Sci. Lett.*, *194*, 241–257.

Charlou, J. L., Y. Fouquet, J. P. Donval, J. M. Auzende, P. Jean-Baptiste, M. Stievenard, and S. Michel (1996), Mineral and gas chemistry of hydrothermal fluids on an ultrafast spreading ridge: East Pacific Rise, 17° to 19°S (Naudur cruise, 1993) phase separation processes controlled by volcanic and tectonic activity, *J. Geophys. Res.*, *101*, 15,899–15,919.

Charlou, J. L., J. P. Donval, E. Douville, P. Jean-Baptiste, J. Radford-Knoery, Y. Fouquet, A. Dapoigny, and M. Stievenard (2000), Compared geochemical signatures and the evolution of Menez Gwen (37°50′N) and Lucky Strike (37°17′N) hydrothermal fluids, south of the Azores Triple Junction on the Mid-Atlantic Ridge, *Chem. Geol.*, *171*, 49–75.

Chase, M. W., Jr. (1998), *NIST-JANAF Thermochemical Tables*, 4th ed., *J. Phys. Chem. Ref. Data Monogr.*, vol. 9 (Part II), p. 1343, Am. Inst. of Phys., Melville, N. Y.

Chourabi, B., and J. J. Fripiat (1981), Determination of tetrahedral substitutions and interlayer surface heterogeneity from vibrational spectra of ammonium in smectites, *Clays Clay Miner.*, *29*, 260–268.

Erzinger, J., and W. Bach (1996), Downhole variation of nitrogen in Hole 504B: Preliminary results, *Proc. Ocean Drill. Program Sci. Results*, *148*, 3–7.

Exley, R. A., S. R. Boyd, D. P. Mattey, and C. T. Pillinger (1987), Nitrogen isotope geochemistry of basaltic glasses: Implications for mantle degassing and structure?, *Earth Planet. Sci. Lett.*, *81*, 163–174.

Fromm, E., and H. Jehn (1968), High temperature nitrogen solubility in molybdenum, *J. Less Common Metals*, *14*, 474–475.

Haendel, D., K. Mühle, H. Nitzsche, G. Stiehl, and U. Wand (1986), Isotopic variations of the fixed nitrogen in metamorphic rocks, *Geochim. Cosmochim. Acta*, *50*, 749–758.

Hall, A. (1989), Ammonium in spilitized basalts of southwest England and its implications for the recycling of nitrogen, *Geochem. J.*, *23*, 19–23.

Hanschmann, G. (1981), Berechnung von Isotopieeffekten auf quantenchemischer Grundlage am Beispiel stickstof fhaltiger Moleküle, *Zfl. Mitt.*, *41*, 19–39.

Honma, H., and Y. Itihara (1981), Distribution of ammonium in minerals of metamorphic and granitic rocks, *Geochim. Cosmochim. Acta*, *45*, 983–988.

Honnorez, J. (1981), The aging of the oceanic crust at low temperature, in *The Sea*, vol. 7, edited by C. Emiliani, pp. 525–588, John Wiley, Hoboken, N. J.

Javoy, M., and F. Pineau (1991), The volatiles record of a "popping" rock from the Mid-Atlantic ridge at 14°N: Chemical and isotopic composition of gas trapped in the vesicles, *Earth Planet. Sci. Lett.*, *107*, 598–611.

Laverne, C. (1983), Occurrence of melanite and aegirine-augite in Deep Sea Drilling Project Hole 504B, *Initial Rep. Deep Sea Drill. Proj.*, *69*, 593–605.

Laverne, C. (1993), Occurrence of siderite and ankerite in young basalts from Galapagos Spreading Center (DSDP Holes 506G and 507B), *Chem. Geol.*, *106*, 27–46.

Laverne, C. (2005), Chemical composition of unusual Ti-hydrogarnets from the deepest volcanic rocks cored in ODP Hole 1256D (Leg 206), *Proc. Ocean Drill. Program Sci. Results*, in press.

Laverne, C., A. Belarouchi, and J. Honnorez (1996), Alteration mineralogy and chemistry of the upper oceanic crust from ODP Hole 896A, Costa Rica Rift, *Proc. Ocean Drill. Program Sci. Results*, *148*, 151–170.

Lindgreen, H. (1994), Ammonium fixation during illite-smectite diagenesis in Upper Jurassic shale, North Sea, *Clay Miner.*, *29*, 527–537.

Martinz, H. P., and K. Prandini (1994), The carburization and nitriding of molybdenum and TZM, *Int. J. Refractory Metals Hard Mater.*, *12*, 179–186.

Marty, B., and F. Humbert (1997), Nitrogen and argon isotopes in oceanic basalts, *Earth Planet. Sci. Lett.*, *152*, 101–112.

Marty, B., and L. Zimmermann (1999), Volatiles (He, C, N, Ar) in mid-ocean ridge basalts: Assessment of shallow-level fractionation and characterization of source composition, *Geochim. Cosmochim. Acta*, *63*, 3619–3633.

Marty, B., M. Lenoble, and N. Vassard (1995), Nitrogen, helium and argon in basalt: A static mass spectrometry study, *Chem. Geol.*, *120*, 183–195.

Miyazaki, A., H. Hiyagon, N. Sugiura, K. Hirose, and E. Takahashi (2004), Solubilities of nitrogen and noble gases in silicate melts under various oxygen fugacities: Implications for the origin and degassing history of nitrogen and noble gases in the Earth, *Geochim. Cosmochim. Acta*, *68*, 387–401.

Nishio, Y., T. Ishii, T. Gamo, and Y. Sano (1999), Volatile element isotopic systematics of the Rodrigues Triple Junction Indian Ocean MORB: Implications for mantle heterogeneity, *Earth Planet. Sci. Lett.*, *170*, 241–253.

Olofsson, G. (1975), Thermodynamic quantities for the dissociation of the ammonium ion and for the ionization of aqueous ammonia over a wide temperature range, *J. Chem. Thermodyn.*, *7*, 507–514.

Pinti, D. L., K. Hashizume, and J. I. Matsuda (2001), Nitrogen and argon signatures in 3.8 to 2.8 Ga metasediments: Clues on the chemical state of the Archean ocean and the deep biosphere, *Geochim. Cosmochim. Acta*, *65*, 2301–2316.

Pironon, J., M. Pelletier, P. de Donato, and R. Mosser-Ruck (2003), Characterization of smectite and illite by FTIR spectroscopy of interlayer NH_4^+ cations, *Clay Miner.*, *38*, 201–211.

Pouchou, J. L., and F. Pichoir (1985), ρ(rZ) procedure for improved quantitative microanalysis, in *Microbeam Analysis*, edited by J. T. Armstrong, p. 104, San Francisco Press, San Francisco, Calif.

Sakai, H., D. J. Des Marais, A. Ueda, and J. G. Moore (1984), Concentrations and isotope ratios of carbon, nitrogen and sulfur in ocean-floor basalts, *Geochim. Cosmochim. Acta*, *48*, 2433–2441.

Sano, Y., and C. T. Pillinger (1990), Nitrogen isotopes and N_2/Ar ratios in cherts: An attempt to measure time evolution of atmospheric $\delta^{15}N$ value, *Geochem. J.*, *24*, 315–325.

Shipboard Scientific Party (2003), Leg 206 summary, *Proc. Ocean Drill. Program Initial Rep.*, *206*, 1–117.

Vanko, D. A., C. Laverne, P. Tartarotti, and J. C. Alt (1996), Chemistry and origin of secondary minerals from the deep sheeted dikes cored during ODP Leg 148, Hole 504B, *Proc. Ocean Drill. Program Sci. Results*, *148*, 71–86.

Vedder, W. (1964), Correlations between infrared spectrum and chemical composition of mica, *Am. Mineral.*, *49*, 736–768.

Vedder, W. (1965), Ammonium in muscovite, *Geochim. Cosmochim. Acta*, *29*, 221–228.

Wilson, D. S. (1996), Fastest known spreading on the Miocene Cocos-Pacific plate boundary, *Geophys. Res. Lett.*, *23*, 3003–3006.

Yokochi, R. (2005), L'azote, le neon et le xenon dans le manteau: Sources, processus et heterogeneites, Ph.D. thesis, CRPG, Nancy, France.